Desalination and Water Treatment
www.deswater.com

doi: 10.5004/dwt.2018.23043

130 (2018) 182–193
October

Removal of lead from aqueous solution using low-cost adsorbents from Apiaceae family

Weetara Boontham, Sandhya Babel*

School of Biochemical Engineering and Technology, Sirindhorn International Institute of Technology (SIIT), Thammasat University, Pathum Thani, Thailand, Tel. +662 986-9009 Ext. 2307;
emails: sandhya@siit.tu.ac.th (S. Babel), weetara.boon@gmail.com (W. Boontham)

Received 19 September 2017; Accepted 24 August 2018

ABSTRACT

Adsorbents prepared from the Apiaceae family, namely parsley (PL), coriander (CR), and cilantro (CL), were used for lead (Pb(II)) removal from low-concentration aqueous solutions. Physical and chemical characterizations were carried out by the Brunauer–Emmett–Teller adsorption isotherm, scanning electron microscopy coupled with energy dispersive X-ray analysis, and Fourier transform infrared (FTIR) spectra analysis. Batch experiments were conducted to study the effect of biomass dosage, pH, contact time, agitation speed, and initial lead concentrations. The maximum biosorption of Pb(II) was approximately 89% with 1.0 g/L biomass under an optimum pH of 5 with 2 mg/L initial lead concentration for the three selected adsorbents. The lead removal rate increased with an increase of dosage, speed of rotation, and contact time, while it decreased with a pH greater than 5, and increased initial Pb(II) concentration. The maximum monolayer adsorption capacity of the PL, CR, and CL was 4.48, 2.94, and 3.87 mg/g, respectively. It was found that the Langmuir isotherm provides a good model to describe the adsorption process for PL, CR, and CL. The adsorption process obeyed a pseudo-second-order kinetic model in all cases. Due to its ease of use, local availability, low-cost, and good adsorption capacities, PL, CR, and CL can be used as effective adsorbents for Pb(II) removal from low-concentration aqueous solutions.

Keywords: Biosorption; Green technology; Lead removal; Locally available plants; Low-cost adsorbents; Water remediation

1. Introduction

Access to clean and safe drinking water is a basic right for humans. Water contamination by heavy metals is a major environmental problem due to their acute toxicity and their accumulation in food chains. Lead (Pb) is one of the toxic heavy metals. Lead dissemination can occur naturally in the environment or may be released from industrial residue (batteries, radiators, Pb-based solder joints, etc.). The World Health Organization (WHO) suggests that the tolerance limit for lead concentration in drinking water is 0.01 mg/L [1]. This limit is less than 0.05 mg/L limit by the Thailand Pollution Control Department [2]. Moreover, the limit of lead discharge for wastewater in Thailand is 0.2 mg/L. Hence, this toxic metal must be eliminated as much as possible from effluents to protect the environment and human health.

According to environmental protection legislation and public documents, lead and other toxic heavy metals can be removed from wastewater by conventional techniques, such as chemical precipitation, membrane filtration, reverse osmosis, electrocoagulation, chelation, and ion exchange [3]. However, these methods are often inefficient and/or very expensive for low concentrations of metals. Therefore, there is a need for sought cheaper metal removal technologies that can be applied to low-concentration aqueous systems. In such sense, green technologies based on biosorption processes can be used for pollutant removal from waters, especially those that are not easily biodegradable such as metals. These techniques involve physicochemical and metabolically

* Corresponding author.

independent processes based on a variety of mechanisms, including absorption, adsorption, ion exchange, surface complexation, and precipitation. In general, biotreatment processes are more efficient for pollutants removal from dilute solutions. The most popular adsorbents for heavy metal removal from aqueous solutions are zeolites, activated carbon (AC), silica gel, and chitosan [4]. Although the use of commercially available adsorbents is still very widespread, these materials are very expensive. Recently, biosorption of contaminants by sorbents of natural origin has gained more attention because of several factors, such as free availability, low cost, good adsorption capacity, easy of chemical modification, easy renewal, and fewer disposal problems after adsorption. Natural sorbents are very effective in removing heavy metals even in low concentrations [5].

Plant materials such as *Prosopis juliflora* DC seed [6], peach and apricot stones [7], *Pinus sylvestris* [8], green algae *Spirogyra* species [9], rice husk and maize cobs [10], sago waste [11], brown seaweed *Sargassum filipendula* [12], sawdust (*Acacia arabica*) [13], baobab (*Adononsia digitata*) fruit shells [14], mango tree (*Mangifera indica*) sawdust [15], sop seeds [16], spent tea leaves [17], palm kernel shell charcoal [18], fungus [19], orange barks [20], and peat [21] have been studied for Pb(II) removal from aqueous systems.

At present, much effort has been taken to remove Pb(II) by adsorption, and it is still highly desirable to develop novel adsorbents with high adsorption capacities. However, this is still a big challenge to remove the low-concentration lead ions from water. Therefore, the main objective of this study was to develop a method based on the use of parsley (PL), coriander (CR), and cilantro (CL) plants as a potential biosorbent for the removal and determination of lead ions in polluted aqueous solutions. Preliminary results using PL, CR, and CL also indicated that these biosorbents can be effectively used to adsorb Pb(II) from synthetic water [22]. In this study, the physical and chemical characteristics of the selected adsorbents were examined in terms of specific surface area, surface physical morphology and composition, and surface functional groups. A series of batch adsorption experiment was performed to determine the influence of biomass amount, pH, agitation speed, contact time, and initial Pb(II) concentration. Furthermore, the obtained data were evaluated and fit using adsorption isotherms and kinetic models to understand the mechanisms involved in the adsorption process.

2. Materials and methods

2.1. Materials and reagents

A stock solution of lead containing 100 mg Pb^{2+}/L was prepared by dissolving 79.95 mg of $Pb(NO_3)_2$ in deionized water. Then 5 mL of HNO_3 was added. This was diluted to 500 mL with deionized water. By using this stock solution, other standard solutions were prepared at different Pb(II) concentrations. Hydrochloric acid (1 N) and/or 1 N sodium hydroxide (1 N) were used for pH adjustment.

2.2. Preparation of adsorbents

PL, CR, and CL are classified in the Apiaceae family. Plants in this family are mostly aromatic flowering plants and have been widely used in cooking. PL is cultivated in the northern region of Thailand as it requires special cultivation. PL grows best in moist conditions between 22°C and 30°C, in well-drained soil, with full sun. CR and CL are widely cultivated in all regions of Thailand and are easy to obtain. The experiments in this study were performed using all parts of the PL, CR, and CL to produce the lead removal adsorbents without chemical additives. PL, CR, and CL in this study were bought from a local market. The plants were preliminary washed with tap water to remove any pulpy residues. Then, they were cut into small pieces, crushed, and washed thoroughly with deionized water, to eliminate any adhering dirt. To obtain dried adsorbent particles, the plants were then dried overnight in an oven at 90°C to remove any residual moisture. Sunlight can also be used in a small community or a rural area. After that, the dried plants were ground and sieved through a 250-mesh sieve. The powdered plants were stored in an air-tight container for further use.

2.3. Characterization of adsorbents

The physical and chemical properties of the prepared adsorbents were investigated. Surface area characterization was performed using a Micromeritics 3Flex Surface Characterization Analyzer, using nitrogen adsorption based on Brunauer–Emmett–Teller (BET) theory. Degas conditions were done under vacuum with an initial heating rate of 10°C/min up to a temperature of 110°C, kept for a minimum of 9 h. The analysis was done using OMNIC software version 9.2. The adsorbent surface morphology and wt. % of elements was studied by SEM-EDX (scanning electron microscopy coupled with energy dispersive X-ray; JEOL Model JSM-5410) under high vacuum. The experiment was carried out by the bombardment of electrons on a target sample. The sample was spread over a 10-mm aluminum stub with the help of carbon adhesive doubled edged tape. Then the surface was coated with gold foil using a gold-coating machine (Fison Instruments Polaron SC7640). The electrons interact with atoms in the sample, producing various signals containing information of a sample's surface topography. The functional groups were analyzed by IR spectroscopy using a Thermo Scientific Nicolet iS50 FTIR spectrometer. A small amount of adsorbent (in grams) was ground and mixed with spectral-grade KBr in a ratio of 1:10, and pressed under high vacuum pressure to obtain a transparent pellet. The Fourier transform infrared (FTIR) data were collected from 4,000 to 400 cm^{-1} at 1 cm^{-1} resolution.

2.4. Batch adsorption equilibrium experiments

Batch equilibrium tests were performed to investigate the Pb(II) adsorption on PL, CR, and CL. Experiments were performed in 125 mL conical flasks with 50 mL of test solution at room temperature (25 ± 2°C). The effects of adsorbent biomass (0.1, 0.5, 1, 2, and 4.0 g), pH of the solution (2, 3, 4, 5, 6, 7, 8, 9, and 10), agitation speed (100, 150, 200, 250, and 300 rpm), contact time (10, 20, 30, 40, 50, 60, 120, 180, and 360 min), and initial Pb(II) concentration (2, 4, 6, 8, and 10 mg/L) were studied. During the experiments, the parameter under study was varied while the others were kept constant. At the end of the desired contact time, the conical flasks were removed from the rotary shaker, and the adsorbent was allowed to

decant for 2–3 min. Finally, the samples were filtered using Nylon Syringe Filters, 0.22 μm, 13 mm in diameter. The filtrates were analyzed for residual Pb(II) concentration using an inductively coupled plasma spectrometer (Optima 8000, Perkin Elmer). The percentage of Pb(II) removal was calculated by Eq. (1) as follows:

$$\text{Removal}(\%) = \frac{C_0 - C_t}{C_0} \times 100 \quad (1)$$

where C_0 and C_t are the initial and the final Pb(II) concentration (mg/L) at time t, respectively.

The adsorption at equilibrium, q_e (mg/g), was calculated from the mass balance equation as follows:

$$q_e = \frac{C_0 - C_e}{m} \times V \quad (2)$$

where C_0 and C_e are the initial and the final (equilibrium) Pb(II) concentrations (mg/L), respectively. V is the adsorbate volume (L) and m is the mass of the adsorbent used (g) [23].

2.5. Adsorption isotherms

Modeling of adsorption data is essential for predicting and comparing the adsorption performance. This is critical for the optimization of the adsorption mechanism pathways, expression of the adsorbents capacities, and the effective design of adsorption systems [24]. The batch equilibrium experimental data of PL, CR, and CL were fit and analyzed via commonly used models, namely Langmuir and Freundlich isotherms. This study was carried out at room temperature (25 ± 2°C) using variable Pb(II) concentrations of 1–8 mg/L at pH 5 with adsorbent biomass: 1 g/L, agitation speed: 170 rpm, and contact time: 2 h.

2.5.1. Langmuir isotherm

The Langmuir adsorption isotherm model assumes that the adsorption occurs in a homogeneous surface monolayer containing a finite number of adsorption sites. The linear form of the Langmuir adsorption isotherm is given in Eq. (3) as follows:

$$\frac{C_e}{q_e} = \frac{1}{bQ_0} + \frac{C_e}{Q_0} \quad (3)$$

where C_e is the equilibrium Pb(II) concentration (mg/L), q_e is the amount of Pb(II) adsorbed per unit mass of adsorbent (mg/g), and Q_0 and b are Langmuir constants related to the monolayer adsorption capacity (mg/g) and adsorption rate (L/mg), respectively. Values of Q_0 and b are calculated from a plot of C_e/q_e versus C_e, which gives a straight line with a slope of $1/Q_0$ and an intercept of $1/bQ_0$ [25,26].

The important features of the Langmuir isotherm can be explained in terms of the equilibrium parameter (R_L), which is a dimensionless constant referred to as the separation factor or equilibrium parameter.

$$R_L = \frac{1}{1 + bC_i} \quad (4)$$

where C_i is the highest initial Pb(II) concentration (mg/L) and b is the reciprocal of the concentration at which half saturation of adsorbent is achieved. The R_L value represents the adsorption nature. It is unfavorable if R_L is greater than 1, linear if R_L is equal to 1, favorable if R_L is between 0 and 1, and irreversible if R_L is equal to 0 [26,27].

2.5.2. The Freundlich isotherm

The Freundlich isotherm is applicable to adsorption processes that occur on heterogeneous surfaces. This isotherm gives an expression which defines the surface heterogeneity and the exponential distribution of active sites and their energies [28]. The linear form of the Freundlich adsorption isotherm is given in Eq. (5) as follows:

$$\log q_e = \log K_F + \frac{1}{n} \log C_e \quad (5)$$

where C_e is the equilibrium Pb(II) concentration (mg/L) and q_e is amount of Pb(II) adsorbed per unit mass of adsorbent (mg/g). K_F and n are the Freundlich constants, consolidating the factors affecting the adsorption capacity and the degree of nonlinearity between the solute concentration in the solution and the amount adsorbed at equilibrium, respectively. The values of n and K_F were obtained from the slope and intercept of plots of log q_e versus log C_e. The constant K_F is an approximate indicator of adsorption capacity, while $1/n$ is a function of the strength of adsorption in the adsorption process. If $1/n$ is below 1, this indicates a normal adsorption. In contrast, $1/n$ above 1 indicates cooperative adsorption [28,29].

2.6. Adsorption kinetics

Adsorption parameters are important physicochemical parameters to evaluate the basic qualities of a good adsorbent (such as whether the adsorbent adsorbs metals) [30]. In this study, pseudo-first-order and pseudo-second-order kinetic models were employed to describe the kinetic adsorption process. Kinetic parameters were estimated from the batch adsorption of 2 mg/L Pb(II) at pH 5 at room temperature (25 ± 2°C). The time was varied from 10 to 360 min. The adsorbent biomass was 1 g/L and the agitation speed was 170 rpm.

2.6.1. Pseudo-first-order equation

The pseudo-first-order expression of Lagergren is a widely used kinetic model for adsorption data analysis. This kinetic model is used for a reversible reaction with an equilibrium being established between liquid and solid phases, as in Eq. (6):

$$\log\left(q_e - q_t\right) = \log q_e - \frac{k_1 t}{2.303} \quad (6)$$

where q_e and q_t are the amounts of Pb(II) adsorbed (mg/g) at equilibrium and at time t, respectively, and k_1 is the adsorption rate constant of pseudo-first-order adsorption (min^{-1}). A plot of $\log(q_e - q_t)$ versus t gives a straight line. The rate constant k_1 (min^{-1}) is calculated from the slope of the linear plot [31,32].

2.6.2. Pseudo-second-order equation

The pseudo-second-order equation is utilized for a two-site-occupancy adsorption system. In this model, the rate-limiting step is the surface chemisorption, where the removal from solution is due to physicochemical interactions between the two phases, occurring at the same time. The pseudo-second-order adsorption kinetic model is expressed in Eq. (7) as follows:

$$\frac{1}{q_t} = \frac{1}{k_2 q_e^2} + \frac{1}{q_e} t \tag{7}$$

where k_2 (g mg^{-1} min^{-1}) is the rate constant of the pseudo-second-order kinetic equation, and q_e and q_t are the amounts of Pb(II) adsorbed (mg/g) onto selected adsorbents at equilibrium and at time t, respectively. The rate constant k_2 (g mg^{-1} min^{-1}) and equilibrium adsorption capacity q_e were calculated from the slope and intercept of the linear plot of t (time) versus t/q_t [31].

If the kinetic model fits the pseudo-first-order reaction, this suggests that the adsorption system corresponds to a diffusion-controlled process, and the reaction is inclined toward physisorption. Likewise, if the reaction fits the pseudo-second-order model, this shows that the adsorption mechanism is predominant, and the overall rate of the metal adsorption process is controlled by the chemical process [33–35].

3. Result and discussion

3.1. Characterization of prepared adsorbents

3.1.1. BET surface area and pore volume

The specific surface area of an adsorbent, a key factor in the effectiveness of a sorbent, was calculated with the BET adsorption isotherm using nitrogen as the adsorbate [36]. As shown in Table 1, PL, CR, and CL diameters are classified as mesopores, according to the IUPAC classification [37]. CR has the highest surface area, followed by CL and PL. As the specific area of the adsorbents that are 75.42, 88.76, and 75.93 m^2/g, respectively. Their average mean pore diameters are very small, approximately 5 nm. BET analysis shows that PL, CR, and CL do not have a high surface area as compared with commercially available adsorbents, such as AC (1,688 m^2/g) and carbon nanotubes (177 m^2/g). However, it is higher than the more expensive graphene oxide (32 m^2/g) based adsorbents [25]. The surface area of all the adsorbents employed in this study is small when compared with other commercially available adsorbents. However, the surface area is not the only factor that affects the adsorption capacity of an adsorbent. It also depends on other factors such as the presence of surface functional groups on the adsorbents and the experimental conditions.

3.1.2. SEM analysis

SEM analysis was employed to determine the surface characteristics of the prepared samples and metal loaded samples, to perceive the impact of Pb(II) sorption on the surface of the adsorbents. SEM analysis revealed that there were significant changes on the surface of the adsorbents after interaction with Pb(II) ions. The surface morphology of adsorbents before adsorption was irregular and rough, as shown in Fig. 1. After the adsorption of Pb(II), PL showed a carpet-like surface with heterogeneous and disarrangement grooves on its surface, suggesting agglomeration or clustering due to the stress produced by the agitation during the experiment [38]. CR and CL exhibited somewhat changed morphology. Loss of surface porosity, roughness, and numerous cavities were noticeable. Due to the small amount of adsorbed lead (3.8–4.5 mg/g), lead precipitates were not visible on the surface of the adsorbent. In addition, the zoom on the images should be greater, as the size of the lead precipitates are well below 1 μm (nanometric scale).

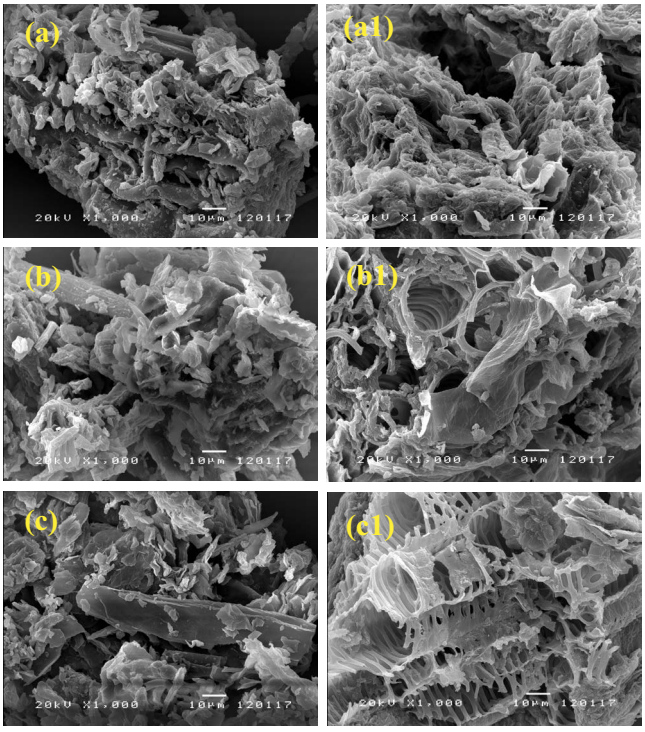

Fig. 1. SEM images of (a) PL, (b) CR, and (c) CL, before (left) and after (a1, b1, and c1) sorption of Pb(II) (1,000×).

Table 1
BET surface areas and pore characteristics of prepared adsorbents

Adsorbents	BET surface area (m^2/g)	Total pore volume (cc/g)	Mean pore diameter (nm)
PL	75.42	0.1560 at P/P_0 = 0.996	4.61
CR	88.76	0.1556 at P/P_0 = 0.994	4.72
CL	75.93	0.1560 at P/P_0 = 0.996	4.65

3.1.3. EDX analysis

EDX analysis was performed to determine the elemental composition of the biosorbents before and after Pb(II) adsorption. The EDX analysis in Fig. 2 shows the chemical composition of the biomass. The EDX spectra depict the peaks of C, O (H could not be measured), K, and Ca, which are the main components of cellulose and lignin that are present in the biomass. These peaks show the available functionalities on the biomass, such as carboxylic acid (–COOH) and hydroxyl group (–OH). Furthermore, the changes of C and O atomic concentrations after Pb(II) adsorption confirmed that lead(II) can covalently bond with C- and O-functional groups such as carboxylate and hydroxyl, which are able to attract and bond with Pb(II) [18]. Since the amount of Pb(II) adsorbed on the biomass is small, no peaks of Pb(II) can be observed after adsorption (Figs. a1, b1, and c1). In conclusion, it can be assumed that the small amount of Pb(II) absorbed and the preparation of the samples for subsequent visualization may have affected the results of the SEM-EDX analysis. Results also suggest that some functional groups may be participating in the process, which is additionally confirmed by FTIR analysis.

3.1.4. FTIR analysis

Infrared spectroscopy is an important tool to determine the influence of surface functional groups that are involved in the interactions with metal ions. The adsorption capacity of an adsorbent is dependent on the chemical reactivity of functional groups on the adsorbent surface [40]. Therefore, FTIR analysis was carried out for the prepared adsorbents in this study. The FTIR spectra of PL, CR, and CL adsorbents before and after adsorption display a number of absorption bands which imply the presence of various functional groups in the biomass, as shown in Fig. 3. The functional groups favorable for Pb(II) adsorption are listed in Table 2. The spectra reveal 11 explicit bands in the wavenumber range of 4,000–400 cm^{-1}. The FTIR spectrum of raw adsorbents shows an abundance of carboxyl and hydroxyl groups which are commonly present in the biomass and may act in deprotonated forms as key sites for coordination of heavy metals. Furthermore, after the adsorption of Pb(II) (Table 2), it can be confirmed that carboxyl, hydroxyl, amide, and amino functional groups play a major role in Pb(II) binding and can combine with Pb(II) as there are obvious changes in the spectra, C–H, CH_2, C=O, and C-Br bending vibrations play a minor role in Pb(II) complexes as shown by the slight changes in the corresponding peak wavenumbers [41,42]. Fig. 3(b) represents FTIR spectra after the adsorption of Pb(II). There is a shift in the position of the peaks after Pb(II) adsorption. These shifts may be attributed to the changes in counter ions associated with carboxylate and hydroxylate anions, suggesting that oxygen-containing acidic functional groups, carboxyl and hydroxyl, are predominant contributors to Pb(II) ion uptake for the adsorption of Pb(II) ions on the surface of an adsorbent [43].

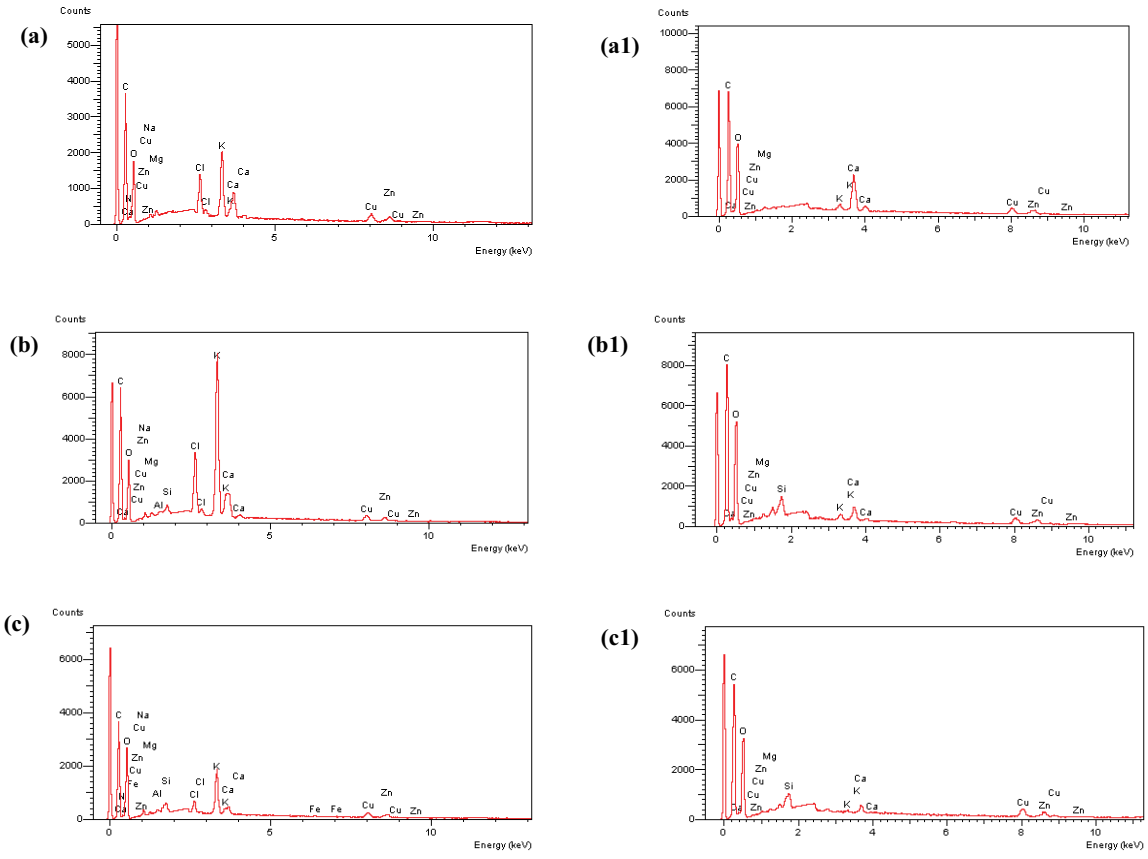

Fig. 2. Characteristic of EDX spectra of (a) PL, (b) CR, and (c) CL, before and after sorption (a1, b1, and c1) of Pb(II), respectively.

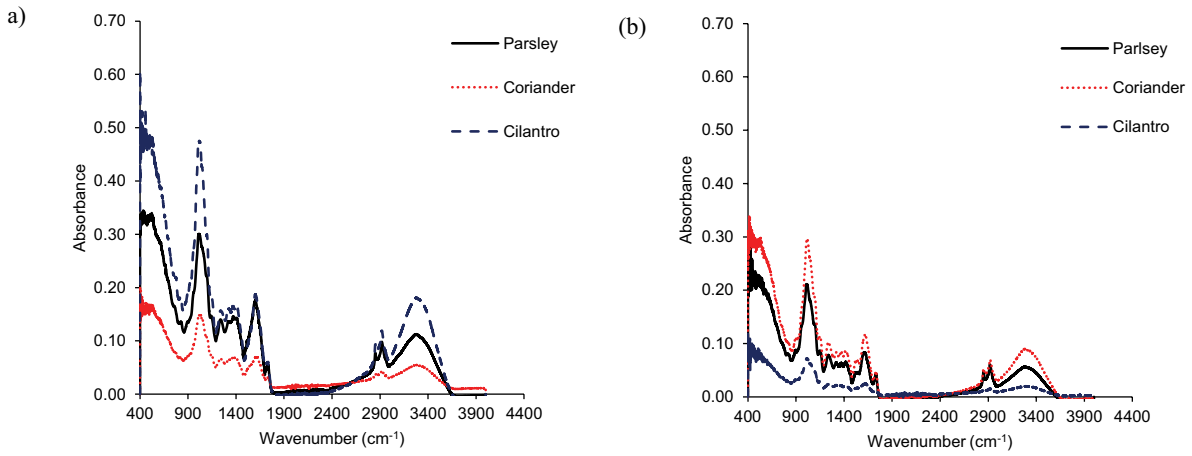

Fig. 3. FTIR spectra of PL, CR, and CL (a) before and (b) after adsorption of Pb(II).

Table 2
FTIR spectroscopic band assignment of surface functional groups on PL, CR, and CL

Wavenumber (cm^{-1}) before adsorption			Wavenumber (cm^{-1}) after adsorption			Functional group	Ref.
PL	CR	CL	PL	CR	CL		
3,278.19 (Broad band)	3,273.95 (Broad band)	3,279.50 (Broad band)	3,271.87 (Broad band)	3,279.69 (Broad band)	3,291.71 (Broad band)	Amine (–NH) and hydroxyl (–OH) stretching vibrations of plant proteins and phenols	[45]
2,918.25	2,920.29	2,918.36	2,918.69	2,920.09	2,920.39	Aliphatic C–H group	
2,850.09	2,851.19	2,850.42	2,851.05	2,851.08	2,848.89	Symmetrical CH_2 stretching band	
1,731.48	1,733.51	1,734.40	1,732.15	1,734.35	1,734.08	C=O stretching, which originates from nonionic carboxyl groups (–COOH, $–COOCH_3$), and may be denoted by carboxylic acids or corresponding esters	[39]
1,604.08	1,616.51	1,600.99	1,610.69	1,622.96	1,616.85	C=O stretching vibrations (from amide I of proteins)	[45]
1,369.95	1,370.71	1,315.66	1,316.40	1,317.75	1,318.61	C–N stretching of aromatic amino group	
1,237.36	1,235.75	1,238.14	1,237.97	1,236.11	1,231.18	C=O stretching band	
1,014.18	1,029.39	1,010.34	1,010.66	1,016.71	1,010.91	Existence of stretching vibrations of C–O of alcohol groups and carboxylic acids	[39]
824.06	823.91	814.18	898.92	851.89	892.42	Primary and secondary amine (–NH)	[46]
753.60	752.03	748.50	755.86	752.52	757.21	Primary and secondary amine (–NH)	
536.71	533.23	533.25	534.25	532.09	532.35	Alkyl halides, C-Br stretching band	[47]

3.2. Adsorption parameters

3.2.1. Effect of dosage on Pb(II) removal

The effect of the amount of biomass on Pb(II) removal is shown in Fig. 4. The maximum removal of Pb(II) was obtained for an adsorbent dose of 2 g/L. Results show that the percent removal of Pb(II) increased rapidly from 20% to 81%, 39% to 70%, and 28% to 86% (Fig. 4(a)) when the biomass content was augmented from 0.1 to 2 g/L for PL, CR, and CL, respectively. Pb(II) removal efficiency increases with increasing adsorbent dose due to the greater availability of exchangeable sites or number of adsorption sites on the surface, and hence, results in a higher percentage of Pb(II) removal [48]. However, Pb(II) adsorption did not increase by further increasing the adsorbent dose which led to a decrease in the percent removal of Pb(II). This decline was a result of an increase in adsorbent density, which causes an aggregation on adsorption sites, limiting the capacity for effective adsorption [49]. Considering the adsorption capacity, a reverse trend was recorded, where a decrease in the adsorption capacity with an increase in adsorbent dose was noticed. This may be the result of a decrease in the total adsorption surface area available for Pb(II) ions to bind due to overlapping or aggregation on adsorption sites at higher dosages. Therefore, as the adsorbent dose increased, the amount of Pb(II) ions adsorbed onto a unit mass of adsorbents decreased, resulting in a decrease in the adsorption capacity [14,50]. To maintain a reasonable capacity and high removal

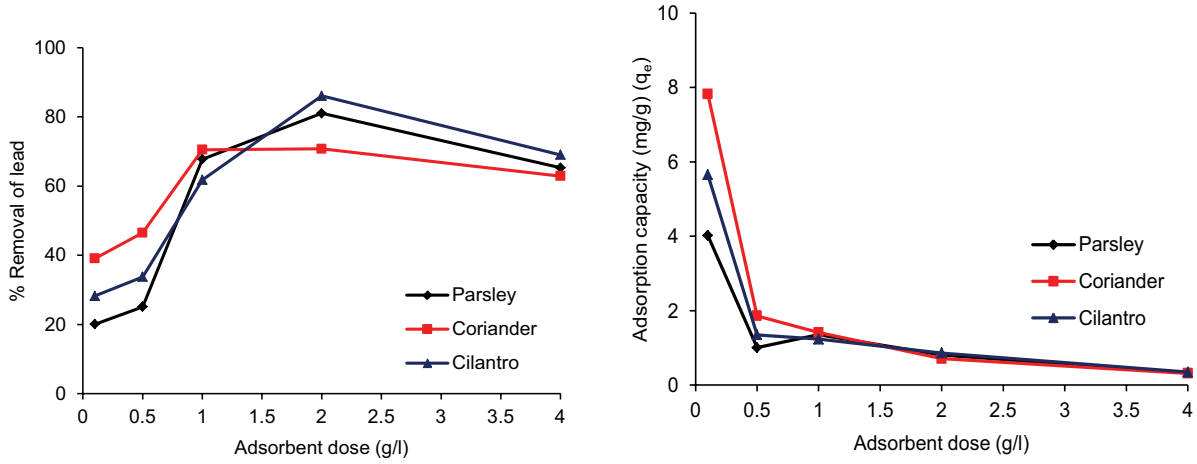

Fig. 4. Effect of adsorbent biomass on (a) Pb(II) removal (%) and (b) adsorption capacity of PL, CR, and CL (initial Pb(II) concentration: 2 mg/L, pH: 5, agitation speed: 170 rpm, contact time: 2 h).

efficiency, the surface loading (i.e., the mass ratio of lead to adsorbent dose) should be lower than the optimum value. Therefore, to ensure effective adsorption at a lower adsorbent dose, 1 g/L is chosen as the applicable dosage for PL, CR, and CL for further adsorption experiments.

3.2.2. Effect of pH on Pb(II) removal

The pH of a solution has a crucial influence on Pb(II) uptake as it determines the surface charge of the adsorbent and the degree of ionization and speciation of an adsorbate during adsorption [51]. The effect of pH on Pb(II) removal is shown in Fig. 5. The adsorption of Pb(II) by PL, CR, and CL was dependent on the pH of the solution, and maximum adsorption was achieved at pH = 5.0. There was an increase in adsorption with increasing pH of solution for Pb(II) ions over a pH range of 2.0–5.0. As the pH increases the number of hydrogen ions in the solution decreases and the number of hydroxide ions increases. These ions are oppositely charged. If they are placed on the active sites of the adsorbent, they can adsorb lead ions. In contrast, at a pH greater than 5.0, adsorption efficiency decreases because hydroxide ions increase in solution. These ions compete with lead ions for being on the active sites of the adsorbent. At a high pH, lead hydroxide ($Pb(OH)_2$) starts to precipitate and deposit in the solution, and thus, this prevents the formation of these ions on the active sites of adsorbent, making true sorption studies difficult [52,53].

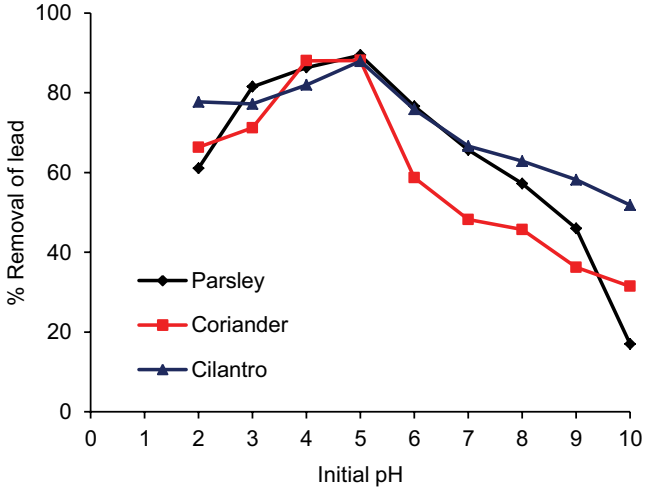

Fig. 5. Effect of pH on Pb(II) removal (%) by PL, CR, and CL (initial Pb(II) concentration: 2 mg/L, adsorbent biomass: 1 g/L, agitation speed: 170 rpm, contact time: 2 h).

Furthermore, at higher pH values, Pb(II) in aqueous solution is converted into different hydrolysis products. Regarding the mechanism of adsorption, an increase of pH of an aqueous solution leads to the hydrolysis of lead species with known equilibrium constant:

$$Pb^{2+} + OH^- \rightarrow PbOH^+, \qquad K_1 = 10^{7.5}$$

$$PbOH^+ + OH^- \rightarrow Pb(OH)_2, \qquad K_2 = 10^{4.5}$$

According to the above reactions, free Pb(II) ions in the adsorption medium were precipitated [52]. Therefore, the adsorption studies cannot be performed at a pH value higher than 5.

In this study, pH 5 was selected because it has been reported that at this value Pb(II) removal was optimum for other plant-based adsorbents, such as activated charcoal [54], *Annona squamosa* shell [55], date palm leaf ash [56], peat [21], rice husk, spent tea leaves, and orange peel [57].

3.2.3. Effect of agitation speed

Agitation speed is an important factor because it affects the outer boundary layer and affects Pb(II) removal. The effect of agitation speed on Pb(II) removal by the selected adsorbents is presented in Fig. 6. The optimum agitation speed was 200 rpm for the three adsorbents. The agitation curve is similar for all the adsorbate–adsorbent systems

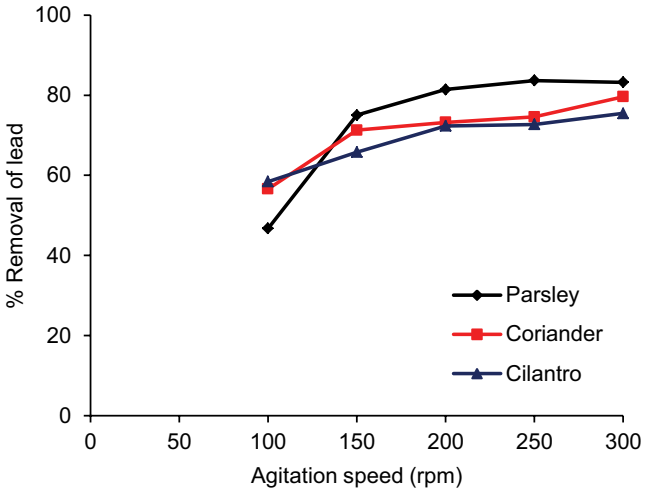

Fig. 6. Effect of the agitation speed on Pb(II) removal (%) by PL, CR, and CL (initial Pb(II) concentration: 2 mg/L, adsorbent biomass: 1 g/L, pH: 5, contact time: 2 h).

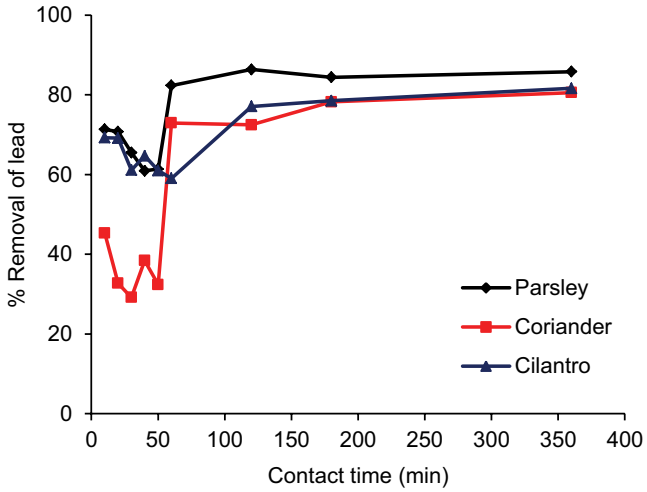

Fig. 7. Effect of contact time on Pb(II) removal (%) by PL, CR, and CL (initial Pb(II) concentration: 2 mg/L, adsorbent biomass: 1 g/L, pH: 5, agitation speed: 170 rpm).

that were studied: with increasing agitation speed, a slight increase in the metal removal occurs. For low agitation (100 rpm), the Pb(II) ions cannot find some active sites on the adsorbents, therefore, the Pb(II) removal was low [58]. The Pb(II) removal increased at a higher stirring rate (beyond 150 rpm). This phenomenon can be explained in terms of the reduction of the boundary layer thickness around the adsorbent particles. Consequently, near the adsorbent surface, the concentrations of Pb(II) ions increase. A higher stirring rate also contributes to a better mass movement of Pb(II) ions from the bulk solution to the surface of the adsorbent and a shortened adsorption equilibrium time [32].

3.2.4. Effect of contact time

It is important to evaluate the effect of contact time required to reach Pb(II) adsorption equilibrium. In most cases, the contact time serves as a reference for the assessment of the residence time required for the adsorption process [59]. The obtained results were plotted as percent removal of Pb(II) against contact time, as shown in Fig. 7. The result shows that the adsorption process takes place in two stages. The first stage is rapid (10–120 min). The second stage after 180 min represents the slow process of adsorption, and the adsorption rate is nearly constant. Therefore, 180 min of contact time was chosen as the optimum equilibration time in this study. The rapid initial adsorption may be attributed to the accumulation of metals on the surface of the adsorbent, due to the availability of a large number of free binding sites. In the later stage, the binding sites became restricted, and the remaining sites were not occupied. This caused the adsorption system to become slower, to reach equilibrium [14].

3.2.5. Effect of initial concentration

The effect of various initial Pb(II) ion concentrations on the adsorption of Pb(II) ion onto three adsorbents is presented in Fig. 8. As seen in this study, the adsorption of Pb(II) is dependent upon the initial concentration. When the initial Pb(II) concentrations were increased from 2 to 10 mg/L, the percentage of adsorption decreased from 84%, 71%, and 77% to 11%, 17%, and 33% for PL, CR, and CL, respectively, at 2 h. The decline in the Pb(II) removal is due to the availability of a smaller number of surface sites on the adsorbents for a relatively larger number of adsorbing species at higher concentrations [60]. In Fig. 8(b), with an increase in Pb(II) concentration, the adsorption capacity of the adsorbents increased. When the initial concentration of Pb (II) was 6 mg/L for PL, CR, and 8 mg/L for CL, the adsorption capacity was 4.8, 3.4, and 3.6 mg/g for PL, CR, and CL, respectively. Thereafter, the adsorption capacity began to decline. The adsorption capacity increase at the initial stage is due to the increased driving force for mass transfer between the aqueous solution of Pb(II) ions and the solid adsorbents. When the concentration of Pb(II) was further increased, the ratio of the initial number of moles of Pb(II) to the available adsorption surface area was higher, and as a result the adsorption capacity was less [61].

3.3. Adsorption isotherms

The equilibrium isotherm data for the adsorption of Pb(II) on selected adsorbents is represented in Figs. 9 and 10, and Table 3.

The results showed that the maximum adsorption capacity was obtained with a value of Q_0 of 4.48, 2.94, and 3.87 mg/g from the Langmuir model and with a value of K_F of 3.07, 1.86, and 2.18 mg/g from the Freundlich model for PL, CR and CL, respectively. The R^2 value is an important parameter for selecting the best isotherm model. A higher R^2 value suggests that the model describes the adsorption data more effectively. Therefore, in this study, the adsorption data are in close agreement with the Langmuir isotherm model, suggesting that the adsorption of Pb(II) onto these adsorbents takes place at specific homogeneous sites and is confined to one-layer adsorption [62]. An R_L value (Fig. 10) of less than 1 indicates that the adsorption data fit the Langmuir isotherm

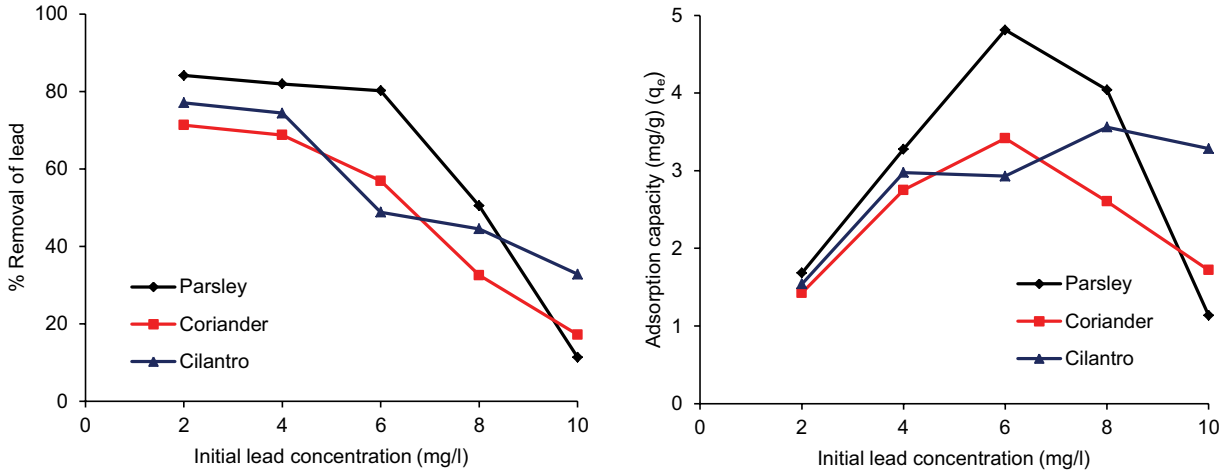

Fig. 8. Effect of initial Pb(II) concentration on (a) Pb(II) removal and (b) adsorption capacity of PL, CR, and CL (adsorbent biomass: 1 g/L, pH: 5, agitation speed: 170 rpm, contact time: 2 h).

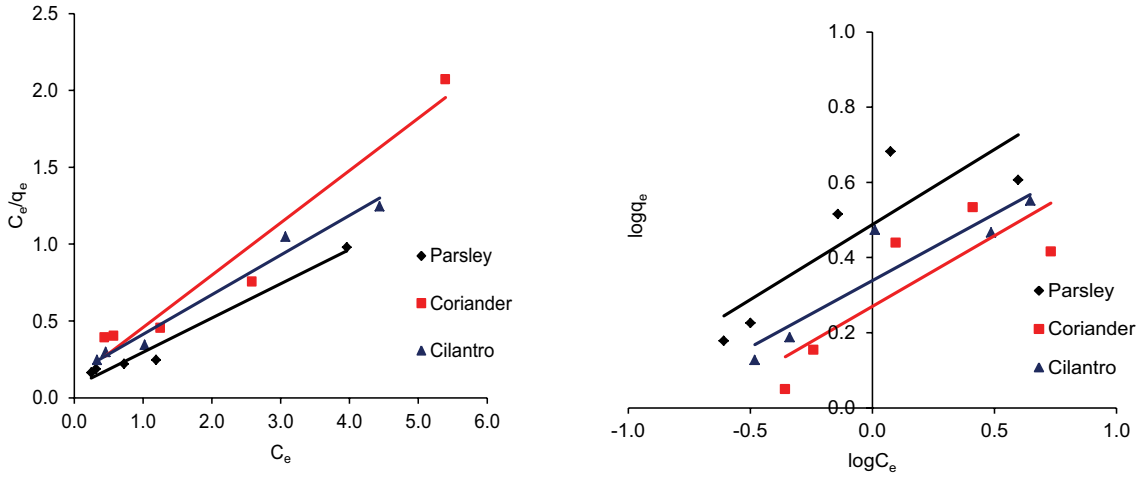

Fig. 9. (a) Langmuir and (b) Freundlich isotherm model for adsorption of Pb(II) onto PL, CR, and CL (adsorbent biomass: 1 g/L, pH: 5, agitation speed: 170 rpm, contact time: 2 h).

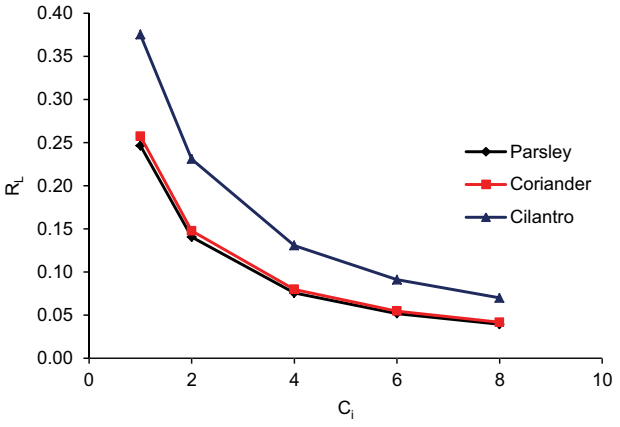

Fig. 10. Separation factor R_L values versus initial Pb(II) concentration (C_i).

model, and the adsorption of Pb(II) onto PL, CR, and CL is favorable [63].

3.4. Adsorption kinetics

The adsorption kinetics explains the Pb(II) removal rate as a function of equilibrium contact time. The linear analysis of adsorption data with two different kinetic models is shown in Fig. 11. The kinetic values are listed in Table 4.

The correlation coefficients for the pseudo-second-order kinetic model were found to be higher than those for the first-order kinetic model, and the calculated q_e values are close to the experimental q_e values. Therefore, the kinetics of Pb(II) adsorption for PL, CR, and CL fits well the pseudo-second-order model, which suggests that chemisorption is the rate-determining step in the adsorption process [32]. This finding also supports the result obtained from FTIR analysis.

Table 3
Comparison of adsorption isotherm parameters of Pb(II) for PL, CR, and CL

Isotherm	Parameters	Adsorbent		
		PL	CR	CL
Langmuir	b (L/mg)	3.060	2.887	1.666
	Q_0 (mg/g)	4.484	2.938	3.873
	R^2	0.975	0.950	0.978
Freundlich	$1/n$	0.400	0.376	0.354
	K_F	3.074	1.863	2.180
	R^2	0.724	0.680	0.848

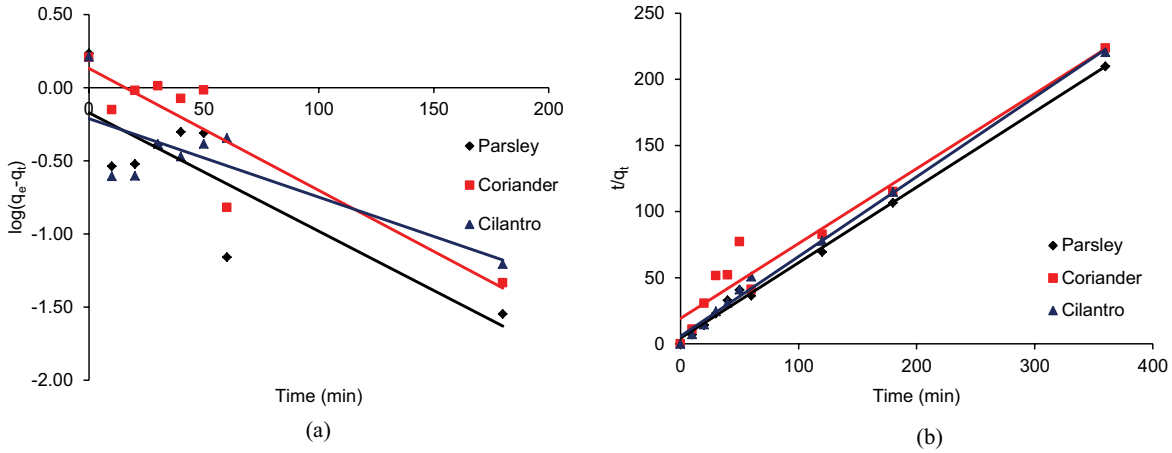

Fig. 11. (a) Pseudo-first-order model and (b) Pseudo-second-order model for adsorption on PL, CR, and CL.

Table 4
Comparison of adsorption kinetic constants of Pb(II) on PL, CR, and CL

Adsorbent	Pseudo-first-order experimental		Pseudo-first-order calculated		Pseudo-second-order calculated		
	q_e (mg/g)	K_1	q_e (mg/g)	R^2	q_e (mg/g)	K_2	R^2
PL	1.716	0.019	1.487	0.695	1.753	0.075	0.996
CR	1.611	0.019	1.356	0.815	1.765	0.017	0.947
CL	1.632	0.012	1.628	0.604	1.659	0.063	0.996

In this case, chemical adsorption can occur by the interactions of the polar functional groups (carboxyl, hydroxyl, amide, and amino) on the adsorbent surface with the metals [44]. Hence, these functional groups are responsible for the sorption of Pb(II) in this study.

4. Conclusion

The present investigation shows that PL, CR, and CL can be employed as potential low-cost adsorbents for the removal of Pb(II) ions from low-concentration contaminated water without any additional chemical and physical treatments. Results show that the Pb(II) removal efficiency of PL, CR, and CL increases with an increase of biomass, contact time, and speed of rotation, whereas the removal rate decreases with an increase of pH beyond 5, and increased initial Pb(II) concentration. Maximum Pb(II) removal efficiency is observed at a biomass dose of 1.0 g/L, pH value of 5, 170 rpm for agitation speed, with 2 h contact time, for the three selected adsorbents.

The physical characterizations support the obtained results. BET analysis indicates that adsorbents are classified as mesopores. SEM-EDX analyses before and after Pb(II) adsorption exhibit the changes in the adsorbent surface during the adsorption process. Although SEM images do not provide evidence of lead biosorption by the biomass, EDX images before and after adsorption suggest that some functional groups are involved in the adsorption of Pb. In addition, FTIR analysis shows that carboxyl, hydroxyl, amide, and amino groups on the surface of the adsorbents played a role in the Pb(II) biosorption. The mechanism of the biosorption of Pb(II) involves surface phenomena such as

chemical adsorption. The equilibrium data are well fit by the Langmuir isotherm model, and the experimental kinetics is pseudo-second-order for PL, CR, and CL. Finally, based on the adsorption results, PL, CR, and CL biomass may be used effectively as an efficient low-cost biomass for the removal of Pb(II) from low-concentration aqueous systems.

Acknowledgment

The authors would like to acknowledge the financial support from the Tokyo Institute of Technology (TAIST-Tokyo Tech), Sirindhorn International Institute of Technology (SIIT), Thammasat University, and the National Science and Technology Development Agency (NSTDA) of Thailand.

References

[1] S. Bachale, S. Sharma, A. Sharma, S. Verma, Removal of lead (II) from aqueous solution using low cost adsorbent: a review, Int. J. Appl. Res., 2 (2016) 523–527.
[2] Thailand Pollution Control Department, Water Quality Standards, Available from: http://www.pcd.go.th/info_serv/en_reg_std_water01.html.
[3] S. Gunatilake, Methods of removing heavy metals from industrial wastewater, J. Multidiscip. Eng. Sci. Technol., 1 (2015) 12–18.
[4] M. Ghaedi, N. Mosallanejad, Removal of heavy metal ions from polluted waters by using of low cost adsorbents, J. Chem. Health Risks, 3 (2013) 7–22.
[5] P.D. Pathak, S.A. Mandavgane, B.D. Kulkarni, Fruit peel waste as a novel low-cost bio adsorbent, Rev. Chem. Eng., 31 (2015) 361–381.
[6] K. Jayaram, M. Prasad, Removal of Pb (II) from aqueous solution by seed powder of *Prosopis juliflora* DC, J. Hazard. Mater., 169 (2009) 991–997.
[7] M. Rashed, Fruit stones from industrial waste for the removal of lead ions from polluted water, Environ. Monit. Assess., 119 (2006) 31–41.
[8] H. Ucun, Y.K. Bayhana, Y. Kaya, A. Cakici, O.F. Algur, Biosorption of lead (II) from aqueous solution by cone biomass of *Pinus sylvestris*, Desalination, 154 (2003) 233–238.
[9] V. Gupta, A. Rastogi, Biosorption of lead from aqueous solutions by green algae *Spirogyra* species: kinetics and equilibrium studies, J. Hazard. Mater., 152 (2008) 407–414.
[10] N. Abdel-Ghani, M. Hefny, G.A. El-Chaghaby, Removal of lead from aqueous solution using low cost abundantly available adsorbents, Int. J. Environ. Sci. Technol., 4 (2007) 67–73.
[11] S. Quek, D. Wase, C. Forster, The use of sago waste for the sorption of lead and copper, Water Sa, 24 (1998) 251–256.
[12] D. Mesquita Vieira, A. da Costa, A. Carlos, C. Assumpção Henriques, V. Luiz Cardoso, F. Pessôa de França, Biosorption of lead by the brown seaweed *Sargassum filipendula*-batch and continuous pilot studies, Electron. J. Biotechnol., 10 (2007) 368–375.
[13] A.K. Meena, K. Kadirvelu, G. Mishra, C. Rajagopal, P. Nagar, Adsorptive removal of heavy metals from aqueous solution by treated sawdust (*Acacia arabica*), J. Hazard. Mater., 150 (2008) 604–611.
[14] F. Chigondo, B.C. Nyamunda, S. Sithole, L. Gwatidzo, Removal of lead (II) and copper (II) ions from aqueous solution by baobab (*Adononsia digitata*) fruit shells biomass, IOSR-J. Appl. Chem., 5 (2013) 43–50.
[15] O.A. Ekpete, E.N. Sor, E. Ogiga, J. Amadi, Adsorption of Pb^{2+} and Cu^{2+} ions from aqueous solutions by mango tree (*Mangifera indica*) saw dust, Int. J. Biol. Chem. Sci., 4 (2010) 1410–1416.
[16] O. Oboh, E. Aluyor, The removal of heavy metal ions from aqueous solutions using sour sop seeds as biosorbent, Afr. J. Biotechnol., 7 (2008) 4508–4511.
[17] A. Yoshita, J. Lu, J. Ye, Y. Liang, Sorption of lead from aqueous solutions by spent tea leaf, Afr. J. Biotechnol., 8 (2009) 2212–2217.
[18] E.A. Oluyemi, A.F. Adeyemi, I.O. Olabanji, Removal of Pb^{2+} and Cd^{2+} ions from wastewaters using palm kernel shell charcoal (PKSC), Res. J. Eng. Appl. Sci., 1 (2012) 308–313.
[19] P. Aytar, S. Gedikli, Y. Buruk, A. Cabuk, N. Burnak, Lead and nickel biosorption with a fungal biomass isolated from metal mine drainage: Box–Behnken experimental design, Int. J. Environ. Sci. Technol., 11 (2014) 1631–1640.
[20] N. Azouaou, Z. Sadaoui, H. Mokaddem, Adsorption of Lead from Aqueous Solution onto Untreated Orange Barks: Equilibrium, Kinetics and Thermodynamics, In: E3S Web of Conferences, EDP Sciences, 2013.
[21] P. Bartczak, M. Norman, Ł. Klapiszewski, N. Karwańska, M. Kawalec, M. Baczyńska, M. Wysokowski, J. Zdarta, F. Ciesielczyk, T. Jesionowski, Removal of nickel (II) and lead (II) ions from aqueous solution using peat as a low-cost adsorbent: a kinetic and equilibrium study, Arabian J. Chem. (2015) 1–14, doi:10.1016/j.arabjc.2015.07.018.
[22] W. Boontham, S. Babel, Apiaceae family plants as low-cost adsorbents for the removal of lead ion from water environment, IOP Conf. Ser.: Mater. Sci. Eng., 216 (2017) 127–131.
[23] O.O. Ogunleye, M.A. Ajala, S.E. Agarry, Evaluation of biosorptive capacity of banana (*Musa paradisiaca*) stalk for lead(II) removal from aqueous solution, J. Environ. Prot., 5 (2014) 1451–1465.
[24] X. Chen, Modeling of experimental adsorption isotherm data, Information, 6 (2015) 14–22.
[25] M.Y. Ali, M.W. Rahman, M. Moniruzzaman, M.J. Alam, I. Saha, M.A. Halim, A. Deb, M.S.A. Sumi, S. Parvin, M.A. Haque, *Nypa fruticans* as a potential low cost adsorbent to uptake heavy metals from industrial wastewater, Int. J. Appl. Bus. Econ. Res., 2 (2016) 1359–1371.
[26] A. Vahid, M. Abdousb, A. MiranBeigia, S. Nayerib, Adsorption and optimization removal of Co $(tsPc)^{-4}$ from aqueous solution using nanoalumina, J. Nanoanal., 3 (2016) 110–119.
[27] K.C.d. Castro, A.S. Cossolin, H.C.O.d. Reis, E.B.d. Morais, Biosorption of anionic textile dyes from aqueous solution by yeast slurry from brewery, Braz. Arch. Biol. Technol., 60 (2017) 9.
[28] N. Ayawei, A.N. Ebelegi, D. Wankasi, Modelling and Interpretation of adsorption isotherms, J. Chem., 2017 (2017) 11.
[29] A. Dada, A. Olalekan, A. Olatunya, O. Dada, Langmuir, Freundlich, Temkin and Dubinin–Radushkevich isotherms studies of equilibrium sorption of Zn^{2+} unto phosphoric acid modified rice husk, IOSR-J. Appl. Chem., 3 (2012) 38–45.
[30] R. Schmuhl, H. Krieg, K. Keizer, Adsorption of Cu (II) and Cr (VI) ions by chitosan: kinetics and equilibrium studies, Water Sa, 27 (2001) 1–8.
[31] H. Radnia, A.A. Ghoreyshi, H. Younesi, Isotherm and kinetics of Fe (II) adsorption onto chitosan in a batch process, IJEEE, 2 (2011) 250–257.
[32] P.S. Kumar, C. Vincent, K. Kirthika, K.S. Kumar, Kinetics and equilibrium studies of Pb^{2+} in removal from aqueous solutions by use of nano-silversol-coated activated carbon, Braz. J. Chem. Eng., 27 (2010) 339–346.
[33] J.-P. Simonin, On the comparison of pseudo-first order and pseudo-second order rate laws in the modeling of adsorption kinetics, Chem. Eng. J., 300 (2016) 254–263.
[34] K. El Ass, F. Erraib, M. Azzi, A. Laachach, Removal of Pb (II) from aqueous solutions by low cost adsorbent, equilibrium, kinetic and thermodynamic studies, J. Mater. Environ. Sci., 9 (2018) 486–496.
[35] T.M.Z.T.K. Azma, A.M.M. Sakinah, A.W. Zularisam, Adsorption and kinetic studies of dyeing *Clitoria ternatea* L. natural dye onto bamboo yarn, Int. J. Eng. Technol. Sci., 7 (2017) 1–16.
[36] C. Barrera-Díaz, M.I.L. Meza, C. Fall, B. Bilyeu, J. Cruz-Olivares, Lead(II) adsorption using allspice-alginate gel biocomposite beads, Sustainable Environ. Res., 25 (2015) 83–92.
[37] M. Thommes, K. Kaneko, A.V. Neimark, J.P. Olivier, F. Rodriguez-Reinoso, J. Rouquerol, K.S. Sing, Physisorption of gases, with special reference to the evaluation of surface area and pore size distribution (IUPAC Technical Report), Pure Appl. Chem., 87 (2015) 1051–1069.
[38] M.I. Sabela, K. Kunene, S. Kanchi, N.M. Xhakaza, A. Bathinapatla, P. Mdluli, D. Sharma, K. Bisetty, Removal of copper (II) from wastewater using green vegetable waste derived activated

carbon: an approach to equilibrium and kinetic study, Arabian J. Chem., (2016) 9, doi:10.1016/j.arabjc.2016.06.001.
[39] D.-L. Mitic-Stojanovic, A. Zarubica, M. Purenovic, D. Bojic, T. Andjelkovic, A.L. Bojic, Biosorptive removal of Pb^{2+}, Cd^{2+} and Zn^{2+} ions from water by *Lagenaria vulgaris* shell, Water Sa, 37 (2011) 303–312.
[40] V.C. Taty-Costodes, H. Fauduet, C. Porte, A. Delacroix, Removal of Cd (II) and Pb (II) ions, from aqueous solutions, by adsorption onto sawdust of *Pinus sylvestris*, J. Hazard. Mater., 105 (2003) 121–142.
[41] D.J. Amorim, H.C. Rezende, É.L. Oliveira, I.L. Almeida, N.M. Coelho, T.N. Matos, C.S. Araújo, Characterization of Pequi (*Caryocar brasiliense*) shells and evaluation of their potential for the adsorption of Pb^{II} ions in aqueous systems, J. Braz. Chem. Soc., 27 (2016) 616–623.
[42] J. Li, Q. Lin, X. Zhang, Y. Yan, Kinetic parameters and mechanisms of the batch biosorption of Cr (VI) and Cr (III) onto *Leersia hexandra* Swartz biomass, J. Colloid Interface Sci., 333 (2009) 71–77.
[43] V. Gupta, A. Rastogi, Equilibrium and kinetic modelling of cadmium (II) biosorption by nonliving algal biomass *Oedogonium* sp. from aqueous phase, J. Hazard. Mater., 153 (2008) 759–766.
[44] M. Iqbal, A. Saeed, S.I. Zafar, FTIR spectrophotometry, kinetics and adsorption isotherms modeling, ion exchange, and EDX analysis for understanding the mechanism of Cd^{2+} and Pb^{2+} removal by mango peel waste, J. Hazard. Mater., 164 (2009) 161–171.
[45] C. Luna, E.D. Barriga-Castro, A. Gómez-Treviño, N.O. Núñez, R. Mendoza-Reséndez, Microstructural, spectroscopic, and antibacterial properties of silver-based hybrid nanostructures biosynthesized using extracts of coriander leaves and seeds, J. Hazard. Mater., 164 (2009) 161–171.
[46] I.U. Khan, W. Dubey, V. Gupta, Preponderance of bioactive medicinal compounds and ATR-FTIR spectroscopy of coriander and mustard floral honey from *Apis mellifera*, Indo. J. Chem., 17 (2017) 376–384.
[47] C. Obi, O. Njoku, Removal of Ni (II) and Pb (II) ions from aqueous solutions by grapefruit (*Citrus paradisi*) mesocarp biomass, J. Appl. Sci. Environ. Manage., 19 (2015) 435–444.
[48] B. Amarasinghe, R. Williams, Tea waste as a low cost adsorbent for the removal of Cu and Pb from wastewater, Chem. Eng. J., 132 (2007) 299–309.
[49] A. Aderibigbe, O. Ogunlalu, O. Wahab, O. Oluwasina, I. Amoo, Adsorption studies of Cu^{2+} from aqueous solutions using unmodified and citric acid–modified plantain (*Musa paradisiaca*) peels, Am. Sci. Res. J. Eng. Technol. Sci., 32 (2017) 64–78.
[50] F.A. Dawodu, K.G. Akpomie, Simultaneous adsorption of Ni (II) and Mn (II) ions from aqueous solution onto a Nigerian kaolinite clay, J. Mater. Res. Technol., 3 (2014) 129–141.
[51] S. Abbaszadeh, S. Wan Alwi, N. Ghasemi, H. Nodeh, C. Colin Webb, I. Muhamad, Use of pristine papaya peel to remove Pb (II) from aqueous solution, Appl. Surf. Sci., 253 (2007) 4727–4733.
[52] S. Erentürk, E. Malkoç, Removal of lead (II) by adsorption onto *Viscumalbum* L.: effect of temperature and equilibrium isotherm analyses, Int. J. Appl. Basic Sci., 9 (2015) 954–1965.
[53] R. Foroutan, H. Esmaeili, M.K. Fard, Equilibrium and kinetic studies of Pb (II) biosorption from aqueous solution using shrimp peel, Int. Res. J. Appl. Basic Sci., 9 (2015) 954–1965.
[54] P. Kumari, Activated charcoal as low cost adsorbent for the removal of lead, Int. Res. J. Eng. Technol., 4 (2017) 1410–1412.
[55] C.P.J. Isaac, A. Sivakumar, Removal of lead and cadmium ions from water using *Annona squamosa* shell: kinetic and equilibrium studies, Desal. Wat. Treat., 51 (2013) 7700–7709.
[56] F. Ghorbani, A. Sanati, H. Younesi, A. Ghoreyshi, The potential of date-palm leaf ash as low-cost adsorbent for the removal of Pb (II) ion from aqueous solution, Int. J. Eng., 25 (2012) 269–278.
[57] K. Goyal, S. Arora, Equilibrium and kinetic studies of adsorption of lead using low cost adsorbents, Indian J. Sci. Technol., 9 (2016) 1–6.
[58] G.Z. Kyzas, Commercial coffee wastes as materials for adsorption of heavy metals from aqueous solutions, Materials, 5 (2012) 1826–1840.
[59] G. Blázquez, F. Hernainz, M. Calero, L. Ruiz-Nunez, Removal of cadmium ions with olive stones: the effect of some parameters, Process Chem., 40 (2005) 2649–2654.
[60] N.D. Tumin, A.L. Chuah, Z. Zawani, S.A. Rashid, Adsorption of copper from aqueous solution by *Elais Guineensis* kernel activated carbon, J. Eng. Sci. Technol., 3 (2008) 180–189.
[61] M. Anis, S. Haydar, A. Jabbar Bari, Adsorption of lead and copper from aqueous solution using unmodified wheat straw, Environ. Eng. Manage. J., 12 (2013) 2117–2124.
[62] A. Khalid, M.A. Kazmi, M. Habib, K. Shahzad, Kinetic & equilibrium modelling of copper biosorption, J. Eng. Technol., 22 (2015) 131–145.
[63] A. Ali, K. Saeed, F. Mabood, Removal of chromium (VI) from aqueous medium using chemically modified banana peels as efficient low-cost adsorbent, Alexandria Eng. J., 55 (2016) 2933–2942.